NRC Research Press

ARTICLE

Creatine loading elevates the intracellular phosphorylation potential and alters adaptive responses of rat fast-twitch muscle to chronic low-frequency stimulation

Charles T. Putman, Maria Gallo, Karen J.B. Martins, Ian M. MacLean, Michelle J. Jendral, Tessa Gordon, Daniel G. Syrotuik, and Walter T. Dixon

Abstract: This study tested the hypothesis that elevating the intracellular phosphorylation potential (IPP = $[ATP]/[ADP]_{free}$) within rat fast-twitch tibialis anterior muscles by creatine (Cr) loading would prevent fast-to-slow fibre transitions induced by chronic low-frequency electrical stimulation (CLFS, 10 Hz, 12 h/day). Creatine-control and creatine-CLFS groups drank a solution of 1% Cr + 5% dextrose, ad libitum, for 10 days before and during 10 days of CLFS; dextrose-control and dextrose-CLFS groups drank 5% dextrose. Cr loading increased total Cr ($P < 0.025$), phosphocreatine (PCr) ($P < 0.003$), and the IPP ($P < 0.0008$) by 34%, 45%, and 64%, respectively. PCr and IPP were 46% ($P < 0.002$) and 76% ($P < 0.02$) greater in creatine-CLFS than in dextrose-CLFS. Higher IPP was confirmed by a 58% reduction in phospho-AMP-activated protein kinase α (Thr172) ($P < 0.006$). In dextrose-CLFS, myosin heavy chain (MyHC) I and IIa transcripts increased 32- and 38-fold ($P < 0.006$), respectively, whereas MyHC-IIb mRNA decreased by 75% ($P < 0.03$); the corresponding MyHC-I and MyHC-IIa protein contents increased by 2.0- ($P < 0.03$) and 2.7-fold ($P < 0.05$), respectively, and MyHC-IIb decreased by 30% ($P < 0.03$). In contrast, within creatine-CLFS, MyHC-I and MyHC-IIa mRNA were unchanged and MyHC-IIb mRNA decreased by 75% ($P < 0.003$); the corresponding MyHC isoform contents were not altered. Oxidative reference enzymes were similarly elevated ($P < 0.01$) in dextrose-CLFS and creatine-CLFS, but reciprocal reductions in glycolytic reference enzymes occurred only in dextrose-CLFS ($P < 0.02$). Preservation of the glycolytic potential and greater SERCA2 and parvalbumin contents in creatine-CLFS coincided with prolonged time to peak tension and half-rise time ($P < 0.01$). These results highlight the IPP as an important physiological regulator of muscle fibre plasticity and demonstrate that training-induced changes typically associated with improvements in muscular endurance or increased power output are not mutually exclusive in Cr-loaded muscles.

Key words: CLFS, myosin heavy chain, SDS-PAGE, real-time RT-PCR, parvalbumin, SERCA1, SERCA2, metabolic reference enzymes, contractile function.

Résumé : Cette étude vérifie l'hypothèse selon laquelle l'augmentation du potentiel de phosphorylation intracellulaire (PPI = $[ATP]/[ADP]_{libre}$) dans les fibres à secousse rapide du jambier antérieur d'un rat par une charge de créatine (Cr) prévient la transition des fibres musculaires de rapides à lentes causée par l'électrostimulation chronique à basse fréquence (CLFS, 10 Hz, 12 h/d). Les groupes recevant la créatine (contrôle et CFLS) boivent *ad libitum* une solution contenant 1 % de Cr et 5 % de dextrose, et ce, 10 jours avant la CFLS et durant les 10 jours de CFLS; les groupes recevant le dextrose (contrôle et CFLS) boivent une solution contenant 5 % de dextrose. La charge de créatine suscite une augmentation de la Cr totale ($P < 0,025$), de la PCR ($P < 0,003$) et du PPI ($P < 0,0008$) de 34 %, 45 % et 64 %, respectivement. Dans le groupe créatine-CFLS, PCr et PPI demeurent plus élevés de 46 % ($P < 0,002$) et 76 % ($P < 0,02$) comparativement au groupe dextrose-CFLS. La diminution de 58 % de phospho-AMPKα(Thr172) ratifie davantage le plus haut PPI ($P < 0,006$). Dans le groupe dextrose-CFLS, les transcrits de MyHC-I et de MyHC-IIa augmentent de 32 et 38 fois respectivement ($P < 0,006$) alors que l'ARNm de MyHC-IIb diminue de 75 % ($P < 0,03$); le contenu protéique de MyHC-I et de MyHC-IIa augmente de 2,0 ($P < 0,03$) et 2,7 fois ($P < 0,05$) respectivement et celui de MyHC-IIb diminue de 30 % ($P < 0,03$). Par contre, dans le groupe créatine-CFLS, l'ARNm de MyHC-I et de MyHC-IIa ne varie pas et l'ARNm de MyHC-IIb diminue de 75 % ($P < 0,003$); le contenu des isoformes correspondants de MyHC ne varie pas dans le groupe créatine-CFLS. On observe aussi une augmentation ($P < 0,01$) des enzymes de référence dans les groupes dextrose-CLFS et créatine-CLFS, mais on observe une diminution réciproque des enzymes glycolytiques de référence que dans le groupe dextrose-CFLS ($P < 0,02$). La préservation du potentiel glycolytique et le contenu plus élevé en SERCA2 et en parvalbumine dans le groupe créatine-CFLS coïncident avec une augmentation des valeurs du temps de montée de la tension de crête ($P < 0,01$). Ces résultats soulignent l'importance du PPI en tant que régulateur physiologique de la plasticité des fibres musculaires et démontrent que les modifications typiques suscitées à l'entraînement par l'amélioration de l'endurance musculaire et l'augmentation de la puissance produite ne sont pas mutuellement exclusives dans les muscles chargés de créatine. [Traduit par la Rédaction]

Mots-clés : CFLS, chaîne lourde de myosine, PAGE en présence de SDS, RT-PCR en temps réel, parvalbumine, SERCA1, SERCA2, enzymes métaboliques de référence, fonction contractile.

Received 18 August 2014. Accepted 27 January 2015.

C.T. Putman. Exercise Biochemistry Laboratory, Faculty of Physical Education and Recreation, University of Alberta, Edmonton, AB T6G 2H9, Canada; The Centre for Neuroscience, Faculty of Medicine and Dentistry, University of Alberta, Edmonton, AB T6G 2E1, Canada.
M. Gallo, K.J.B. Martins, I.M. MacLean, M.J. Jendral, and D.G. Syrotuik. Exercise Biochemistry Laboratory, Faculty of Physical Education and Recreation, University of Alberta, Edmonton, AB T6G 2H9, Canada.
T. Gordon. The Centre for Neuroscience, Faculty of Medicine and Dentistry, University of Alberta, Edmonton, AB T6G 2E1, Canada; Division of Physical Medicine and Rehabilitation, Faculty of Medicine and Dentistry, University of Alberta, Edmonton, AB T5G 0B7, Canada.
W.T. Dixon. Department of Agricultural, Food and Nutritional Science, University of Alberta, Edmonton, AB T6G 2P5, Canada.
Corresponding author: Charles T. Putman (e-mail: tputman@ualberta.ca).

Introduction

Evidence from a number of studies supports the hypothesis that muscle fibre phenotype is regulated by variations in the intracellular energy potential. Correlative data have revealed a strong relationship between a reduction in the muscle fibre energy potential and fast-to-slow fibre type transitions in rabbit models of chronic muscle training. Henriksson et al. (1988) reported that ATP and phosphocreatine (PCr) levels were reduced in rabbit tibialis anterior (TA) muscles undergoing fast-to-slow fibre type transitions induced by chronic low-frequency electrical stimulation (CLFS: 10 Hz, 10 h daily). Building on those observations, Pette et al. (Green et al. 1992; Hämäläinen and Pette 1997) used a similar experimental model to investigate the temporal relationship between the ratio [ATP]/[ADP]$_{free}$, which they termed the intracellular phosphorylation potential (IPP), and related phenotypic adaptations within mixed fast-twitch rabbit TA. They showed that CLFS induced a large decrease in the IPP that preceded (Green et al. 1992) and then paralleled fast-to-slow myosin heavy chain (MyHC) fibre type transitions, increased oxidative potential (Green and Pette 1997), and increased slow sarco(endo)plasmic reticulum Ca^{2+}-ATPase (SERCA2) isoform content (Hämäläinen and Pette 1997). Those phenotypic changes were accompanied by gradual decreases in glycolytic potential, parvalbumin content (Huber and Pette 1996; Carroll et al. 1999), and SERCA1 (fast isoform) protein expression (Hämäläinen and Pette 2001).

Prolonged feeding of the creatine (Cr) antagonist β-guanidine propionate (β-GPA) has been shown to cause a substantial reduction in the IPP in rodent muscles, revealing a causal link between the cellular energy potential and muscle phenotype (Ren et al. 1995; Brault et al. 2003). In those studies, decreases in the muscle IPP resulted in the transition of mixed fast-twitch muscles toward a slower, more oxidative phenotype (Ren et al. 1995). Furthermore, when muscle training was superimposed, the extent of fast-to-slow phenotypic transformation was augmented (Roussel et al. 2000). Further support for the involvement of the IPP in determining muscle phenotype is found in single-fibre studies conducted by Conjard et al. (1998), who reported the IPP was greatest in the fast fibre populations, increasing from IIA to IID(X) to IIB fibres. They also reported that a large CLFS-induced decrease of the IPP occurred within the fast type IID(X) and IIB fibre populations before their transition into slower oxidative type IIA fibres.

Based on those collective observations, we recently investigated whether increasing the cellular energy potential within rat plantaris, by long-term Cr loading, would attenuate fast-to-slow phenotypic transitions typically associated with long-term voluntary wheel running of an intermittent, high-frequency nature (Gallo et al. 2006, 2008). In those studies, prolonged muscle Cr loading attenuated running-induced fast-to-slow fibre type transitions. Although Cr feeding induced a 20% increase in total muscle Cr content (TCr), a corresponding increase in the IPP was not detected in whole-muscle extracts. This was attributed to the phasic, high-frequency nature of voluntary run training facilitating preferential Cr uptake into heavily recruited type IIB fibres (Gallo et al. 2008). Because the IIB population represented only 23% of all fibres in rat plantaris, the maximum increase in whole-muscle IPP was limited to 4.6%.

Thus, the purpose of the present study was to extend our previous work by investigating the effects of maximum Cr loading on the whole-muscle IPP and related phenotypic changes induced by 10 days of CLFS, a critical stimulation period in this model of forced contractile activity that is known to induce the maximum rate of fast-to-slow fibre type transitions (Conjard et al. 1998; Martins et al. 2012). Because fibre contraction is a determinant of Cr uptake (Snow and Murphy 2003), and CLFS imposes the same contraction parameters onto all fibres (Pette and Vrbová 1999), we reasoned that Cr uptake by muscle fibres would be ubiquitous, resulting in greater intracellular Cr accretion. Under these intracellular conditions, the creatine kinase (CK; EC 2.7.3.2) equilibrium favours PCr and ADP production while a linked reaction catalysed by adenylate kinase (AK; EC 2.7.4.3) converts 2 ADP to AMP and ATP, leading to an increase in the [ATP]/[ADP]$_{free}$ ratio (i.e., IPP) (Hardie et al. 1999). Cr loading was achieved by ad libitum drinking of a 1% Cr solution, sweetened with 5% dextrose, for 10 days before and during 10 days of CLFS. Here we report the largest documented increase in TCr to date (i.e., 34%) and an associated 64% increase in the IPP. The novel experimental model employed in our study allowed us to test the hypothesis that increasing the IPP in rat fast-twitch TA muscles would change the adaptive response to CLFS by preventing fast-to-slow MyHC transitions as well as the associated changes in metabolism and the Ca^{2+} regulatory proteins SERCA1, SERCA2, and parvalbumin.

Materials and methods

Animals and care

Twenty-four male Sprague–Dawley rats (237 ± 3.5 g) were used in this study. All experiments were completed in accordance with the guidelines of the Canadian Council on Animal Care. Ethics approval was received from the University of Alberta Health Sciences Animal Welfare and Policy Committee. Animals were individually housed under controlled environmental conditions (22 °C and alternating 12-h light and dark periods); high-protein rat chow and drinking solutions were consumed ad libitum.

Experimental design

Animals were randomly assigned to 1 of 4 treatment groups. Two groups consumed, ad libitum, a solution of 5% dextrose (vehicle) (Fisher Scientific, Fairlawn, N.J., USA); one of those groups received 10 days of CLFS applied to the left hind limb on days 11–20 (dextrose-CLFS, $n = 6$), while the second received a sham operation of the left hind limb (dextrose-control, $n = 5$). Throughout the study the third and fourth groups consumed, ad libitum, a solution of 1% Cr (Createam, NutraSense Inc., Shawnee Mission, Kans., USA) that was sweetened with 5% dextrose to increase palatability and maximise Cr intake (Gallo et al. 2006, 2008). Ten days of CLFS was applied to the left hind limb of the third group (creatine-CLFS, $n = 7$) and the fourth group received a sham operation of the left hind limb (creatine-control, $n = 6$). The right contralateral hind limbs served as internal controls.

Surgery and chronic low-frequency stimulation

CLFS (10 Hz, impulse width 380 μs, 12 h/day) was applied as previously described (Putman et al. 2004, 2007; Martins et al. 2012). While rats were under general anaesthesia, bipolar electrodes were implanted lateral to the common peroneal nerve of the left hind limb, externalised, and connected to a small portable stimulator; animals recovered for 7 days. On days 1 to 10, animals consumed solutions of either 5% dextrose or 5% dextrose + 1% Cr; CLFS was applied on days 11–20.

Measurement of isometric muscle contractile properties

Isometric functional measures were completed according to Gallo et al. (2006). Animals were anaesthetised, incisions were made along the dorsum of the right and left hind limbs, and the ankle tendons of the TA muscles were separated and individually tied with 2.0 silk, while the extensor digitorum longus was denervated. A silastic nerve cuff embedded with 2 multi-stranded stainless steel wires (AS632, Cooner, Chatsworth, Calif., USA) was positioned around the sciatic nerve for electrical stimulation. The 2.0 silk was then attached to a Kulite strain gauge (model KH-102, Kulite Semiconductor Products Inc., Leonia, N.J., USA) for sequential force recordings of maximum twitch force (TW_f, millinewtons), time to peak tension (TTP, milliseconds), half-rise time (½RT, milliseconds), and half-fall time (½FT, milliseconds).

Muscle sampling

Upon completion of each experiment, animals were allowed to recover. TA muscles were collected from anaesthetised animals (75 mg ketamine and 8 mg xylazine per kilogram body weight), weighed, rapidly frozen in melting isopentane cooled in liquid nitrogen (–159 °C), and stored in liquid N_2. Animals were immediately euthanised with Euthanyl (100 mg/kg body weight).

Total muscle creatine content

TA muscles were analysed for TCr (Gallo et al. 2008). Neutralised perchloric acid (PCA) extracts of freeze-dried, powdered TA muscles were added to 1 mol/L nitric acid, boiled for 40 min, cooled to 4 °C, and cleared by centrifugation (12 000*g* for 5 min, 4 °C). Samples were diluted with 1.55 mol/L NaOH, 60 mmol/L Na_2PO_4, and 11.5 mmol/L picric acid, and absorption was read at 513 nm (Ultraspec 3000, Fisher Scientific).

ATP, ADP, PCr, Cr, and [ATP]/[ADP]$_{free}$ (IPP)

Portions of TA muscles stored in liquid N_2 were pulverised under liquid N_2 and dissected free of blood and connective tissue. ATP, ADP, PCr, and Cr were spectrophotometrically (Ultraspec 3000, Fisher Scientific) determined in the neutralised (1 mol/L $KHCO_3$) PCA extracts (Putman et al. 1998). Muscle intracellular water content, calculated according to Cieslar et al. (1998), was 0.659 mL/g wet weight, or 87.3% of total tissue water (0.755 mL/g). [ADP]$_{free}$ was calculated using the CK equilibrium (Cieslar and Dobson 2000; Sahlin and Harris 2011).

Calculation of the mass action ratio ($\Gamma_{MM\text{-}CK}$) and transformed Gibbs free energy of the CK reaction ($\Delta G'_{MM\text{-}CK}$)

A parameter that reflects the accumulation of reaction products relative to substrates in vivo, $\Gamma_{MM\text{-}CK}$, was calculated according to Newsholme et al. (1978) and Newsholme and Crabtree (1979), as summarised in eq. 1.

$$(1)\qquad \Gamma_{MM\text{-}CK} = \frac{[ATP] \times [Cr]}{[ADP] \times [PCr]}$$

The resulting $\Gamma_{MM\text{-}CK}$ value was used to calculate $\Delta G'_{MM\text{-}CK}$ according to Newsholme et al. (1978) and Newsholme and Crabtree (1979), as summarised in eq. 2.

$$(2)\qquad \Delta G'_{MM\text{-}CK} = -RT \ln \frac{K'_{eq}}{\Gamma_{MM\text{-}CK}}$$

where K'_{eq} = 166 when [Mg^{2+}] = 1.0 mmol/L, osmolarity = 250 mOsm/L, pH = 7.0, and R = 8.314 J/(mol·K) at 311 K.

α-subunit phosphorylation (Thr172) of 5′-AMP-activated protein kinase (AMPK)

Western blot analyses of phospho-AMPKα (Thr172) and AMPK-α-pan were conducted as previously described (Putman et al. 2007). Extracts of TA were denatured in reducing buffer (5 min at 95 °C). Protein (87 μg/lane) was resolved on 9% SDS-polyacrylamide gels at 115 V (Mini-PROTEAN 3, Bio-Rad Laboratories, Mississauga, Ont., Canada), electro-transferred onto nitrocellulose membranes (Bio-Rad), stained with Ponceau-S (Sigma-Aldrich, Oakville, Ont., Canada), and photographed (Syngene ChemiGenius, Cambridge, UK). Destained membranes were blocked in Tris-buffered saline (0.1% Tween 20, 5% bovine serum albumin (BSA), pH 7.4), followed by sequential incubations with anti-phospho-AMPKα (Thr172) (1.0 μg/mL; 2531, Cell Signaling Technology, Inc., Danvers, Mass., USA) and horseradish peroxidase (HRP)-labelled anti-rabbit IgG (1.0 μg/mL; PI-1000, Vector Laboratories, Burlington, Ont., Canada); immunoreactivity was visualised with Immobilon Western Chemiluminescent HRP Substrate (Millipore Corp., Billerica, Mass., USA) and quantified (Syngene). Membranes were subsequently stripped and reprobed with anti-AMPK-α-pan (1.0 μg/mL; 07-181, Upstate Cell Signaling Solutions, Lake Placid, N.Y., USA), and total AMPK-α was quantified. Phospho-AMPKα (Thr172) and AMPK-α-pan corresponded to 63 kDa (Precision Plus Protein Prestained Standards, Bio-Rad). All antibodies were diluted in blocking solutions.

Electrophoretic analysis of MyHC isoform content

Quantitative MyHC isoform analyses were completed as previously described (Gallo et al. 2006) using a ChemiGenius imaging system (Syngene).

Western blot analyses of parvalbumin, SERCA1, and SERCA2

Parvalbumin (12 kDa), SERCA1 (110 kDa), and SERCA2 (110 kDa) were quantified as previously described (Gallo et al. 2008). Extracts were prepared as before and 10 μg, 50 μg, or 80 μg loaded per lane for parvalbumin, SERCA1, or SERCA2 on 15% (w/v) (parvalbumin) or 7% (SERCA1 or SERCA2) SDS-polyacrylamide mini-gels (3.5% stacking gel; Mini-PROTEAN 3, Bio-Rad). Resolved proteins were electro-transferred onto polyvinylidene difluoride membranes. Parvalbumin (PBS-Tween 20, 5% skim milk powder, pH 7.4) and SERCA1 or SERCA2 (PBS-Tween 20, 2.5% skim milk powder, 1% BSA, Sigma-Aldrich) membranes were blocked, incubated with anti-parvalbumin (0.1 μg/mL; ab11427, Abcam, Cambridge, Mass., USA), anti-SERCA1 (0.2 μg/mL; ab2818, Abcam), or anti-SERCA2 (0.25 μg/mL; ab2861, Abcam), and developed using HRP-labelled anti-rabbit IgG (0.5 μg/mL; PI-1000, Vector Laboratories), HRP-labelled anti-mouse IgG (0.5 μg/mL; PI-2000, Vector Laboratories), or biotinylated anti-mouse IgG (2.5 μg/mL; BA-2000, Vector Laboratories) with HRP-labelled streptavidin (0.2 μg/mL; 474-3000, KPL, Gaithersburg, Md., USA). The respective internal loading controls were α-actinin (100 kDa) (anti-α-actinin, 7.5 μg/mL, clone EA-53, Sigma; anti-mouse IgG, 0.5 μg/mL, PI-2000, Vector Laboratories), β-actin (42 kDa) (anti-β-actin, 0.5 μg/mL, ab8227, Abcam; biotinylated anti-rabbit IgG, 0.5 μg/mL, BA-1000, Vector Laboratories), and desmin (55 kDa) (anti-desmin, 16 μg/mL, DE-U-10, Sigma; biotinylated anti-mouse IgG, 2.5 μg/mL, BA-2000, Vector Laboratories).

MyHC mRNA analyses by real-time reverse transcriptase polymerase chain reaction (RT-PCR)

Patterns of MyHC isoform expression were analysed at the mRNA level using real-time RT-PCR (Martins et al. 2012). Real-time RT-PCR was performed in duplicate using an ABI 7900HT thermocycler (Applied Biosystems). Fold changes in MyHC isoform expression were determined using the $2^{-\Delta\Delta Ct}$ method and 18S rRNA as the endogenous control. Baseline control values of "1 ± 0" were established for each MyHC isoform as the average $2^{-\Delta\Delta Ct}$ of the right contralateral TA of the dextrose (dextrose-base-control, n = 11) or creatine (Cr-base-control, n = 13) groups. Data are expressed as follows: left-sham/dextrose-base-control (dextrose-control), left-stimulated/dextrose-base-control (dextrose-CLFS), Cr-loaded-left-sham/Cr-base-control (creatine-control), and Cr-loaded-left-stimulated/Cr-base-control (creatine-CLFS). This allowed quantification of experimental effects and the associated variances.

Metabolic reference enzymes

Maximal activities of citrate synthase (CS, EC 2.3.3.1), 3-hydroxyacyl-CoA dehydrogenase (HADH, EC 1.1.1.35), phosphofructokinase (PFK, EC 2.7.1.11), glyceraldehyde-3-phosphate dehydrogenase (GAPDH, EC 1.2.1.12) (Putman et al. 2003, 2004; Gallo et al. 2008), and creatine kinase (CK, EC 2.7.3.2) were measured (Lowry et al. 1978) as previously described.

Statistical analyses

Data are presented as the mean ± SEM. Samples were analysed in duplicate or triplicate. Because ATP, ADP, and [ATP]/[ADP]$_{free}$ did not differ between the right contralateral control and left sham within dextrose groups, or between the right contralateral

Fig. 1. (A) Body weight of Sprague–Dawley rats during creatine (Cr) loading and chronic low-frequency stimulation (CLFS): dextrose-control (empty circle), dextrose-CLFS (empty triangle), creatine-control (filled circle), and creatine-CLFS (filled triangle) groups. (B) Daily fluid volume consumed. (C) Daily Cr intake. (D) Cumulative Cr intake.

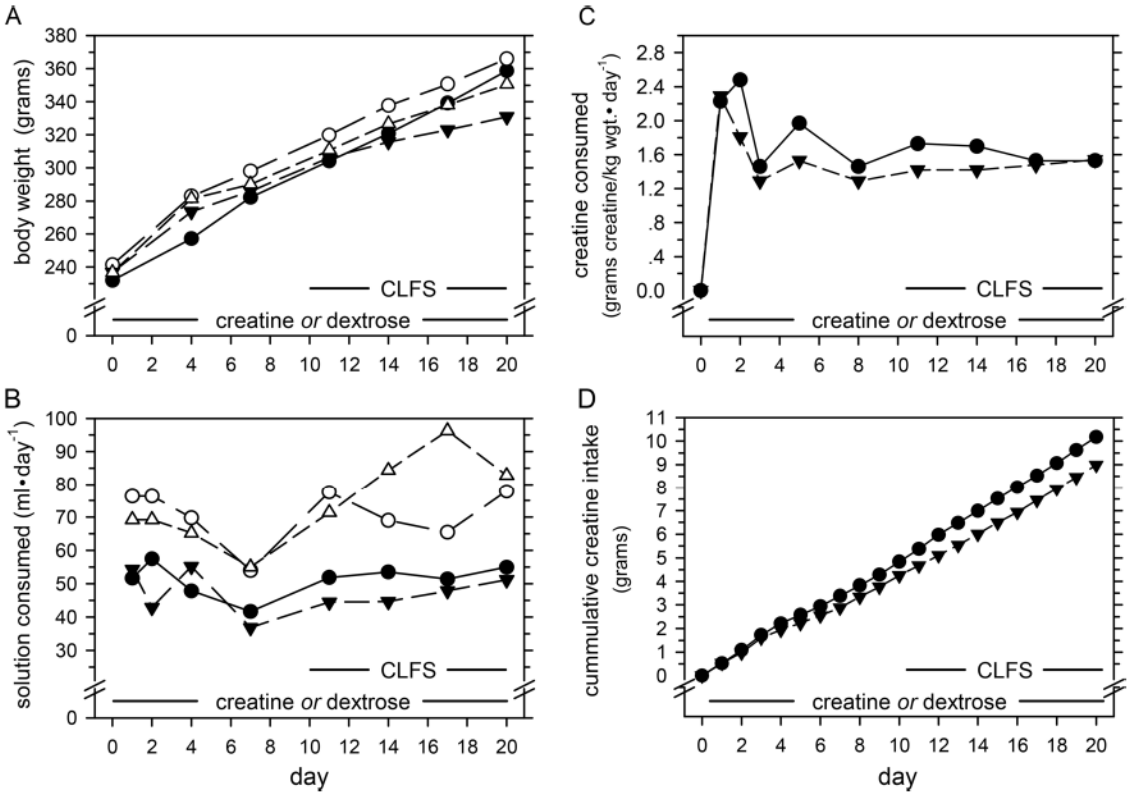

control and left sham within creatine groups, data in Fig. 3 are summarised as follows: dextrose-control (average of right contralateral control and left sham), dextrose-CLFS (CLFS only), creatine-control (average of right contralateral control and left sham), and creatine-CLFS (CLFS only). Data in Figs. 3–5 and 7 are summarised as sham/contralateral control or CLFS/contralateral control. Data were analysed by ANOVA; when a significant *F* ratio was found, differences between group means were compared using Fisher's post hoc analysis for planned comparisons. Data in Fig. 3D were analysed by multivariate regression. Because the direction and magnitude of effects were established a priori for TCr and $[ATP]/[ADP]_{free}$, data were analysed using a one-tailed independent samples *t* test. Differences were considered significant at $P < 0.05$, but *P* values are reported.

Results

Body and muscle mass

Mean body weight increased by 117 ± 5.1 g (Fig. 1A) and did not differ between groups. Average TA weight was 642 ± 10.3 mg and did not differ within rats or between experimental groups.

Solution intake and daily creatine consumption

The total daily volume of solution consumed (Fig. 1B) did not differ between the dextrose-control and dextrose-CLFS groups. Similarly, the total daily fluid volume consumed did not differ between creatine-control and creatine-CLFS. However, rats who drank 5% dextrose consumed 33% more fluid throughout the study than rats who drank 1% Cr + 5% dextrose (1453 ± 429.7 mL vs. 967 ± 121.8 mL, main effect $P < 0.001$; Fig. 1B). At the beginning of the study, Cr intake was 2.2 g/(kg·day) (Fig. 1C), which equated to 7.3 times the recommended human Cr-loading dose of 0.3 g/(kg·day) (Harris et al. 1992). Between 8 and 20 days, Cr intake remained stable at ~1.6 g/(kg·day) (Fig. 1C) and was equivalent to 5.3 times the recommended human Cr-loading dose. Cumulative Cr intake in the present study (Fig. 1D) was 10.2 ± 0.54 g and 9.0 ± 0.56 g for the creatine-control and creatine-CLFS groups, respectively.

Fig. 2. Total creatine (Cr) content within tibialis anterior muscles of dextrose-fed control rats ($n = 11$; dextrose-control and dextrose-CLFS groups) and Cr-fed rats ($n = 13$; creatine-control and creatine-CLFS groups).

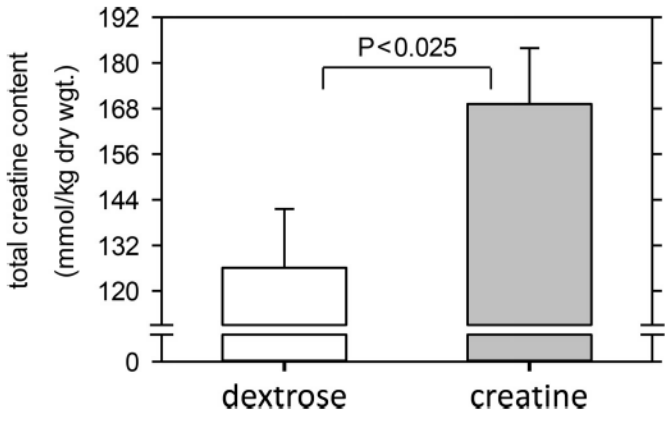

ATP, ADP, TCr, PCr, Cr, and $[ATP]/[ADP]_{free}$ (IPP)

TCr increased by 43 mmol/kg wet weight, or 34%, in Cr-loaded TA muscles (Fig. 2). Ten days of CLFS induced a 22% decrease in ATP content within the dextrose treatment condition (Table 1) but not in Cr-loaded muscles (Table 1). Total muscle ADP contents were not altered by Cr loading or CLFS (Table 1). However, $[ADP]_{free}$ was significantly reduced by Cr loading (main effect $P < 0.002$; Table 1).

Table 1. ATP, ADP, phosphocreatine (PCr), creatine (Cr), and $[ADP]_{free}$ in tibialis anterior muscles of Sprague–Dawley rats.

Treatment	Muscle	ATP	ADP	PCr§	Cr	$[ADP]_{free}$§
Dextrose	Contralateral control	6.77±0.438	1.59±0.148	14.7±1.35	12.40±1.325	56.5±12.71
	Sham	6.71±0.309	1.35±0.128	16.4±1.40	10.28±1.326	41.7±10.21
Dextrose	Contralateral control	6.72±0.453	2.17±0.251	16.3±0.94	13.50±1.683	51.5±7.64
	CLFS	5.24±0.385*,†	1.98±0.174	12.4±1.28*,‡	12.66±0.852	52.8±9.38
Creatine	Contralateral control	6.59±0.402	1.73±0.146	23.6±1.58‡	10.57±0.471	27.0±1.95
	Sham	6.80±0.387	1.74±0.257	22.3±0.72†	10.71±0.684	30.0±2.58
Creatine	Contralateral control	6.76±0.268	1.77±0.220	22.7±0.92	10.72±1.046	29.9±3.89
	CLFS	5.99±0.243	1.85±0.344	18.1±1.23*	10.70±1.046	31.8±2.75

Note: Data are means ± SE. ATP, ADP, PCr, and Cr are expressed as millimoles per kilogram of wet muscle weight. $[ADP]_{free}$ is expressed as micromoles per liter of intracellular water.

*Chronic low-frequency stimulation (CLFS) different from contralateral control ($P < 0.009$).

†Different from creatine-CLFS ($P < 0.02$).

‡Different from creatine-CLFS ($P < 0.002$).

§Creatine loading resulted in decreased $[ADP]_{free}$ and increased PCr (main effect of creatine treatment, $P < 0.005$).

Cr loading induced a 64% increase in $[ATP]/[ADP]_{free}$ (i.e., IPP) within creatine-control compared with dextrose-control ($P < 0.0002$, Fig. 3A). Whereas the IPP was 28% lower in dextrose-CLFS than in dextrose-control (Fig. 3A), it was 30% and 76% higher in creatine-CLFS than in dextrose-control and dextrose-CLFS, respectively (Fig. 3A). Within Cr-loaded muscles, elevation of the IPP resulted from a decrease in resting $[ADP]_{free}$ ($P < 0.002$, main effect) (Table 1) and a preferential 45% increase in PCr (main effect $P < 0.005$; Table 1); the PCr/ATP ratio was elevated by 41% ($P < 0.002$) in Cr-loaded muscles (3.31 ± 0.231) compared with dextrose controls (2.35 ± 0.126).

Calculation of the mass action ratio ($\Gamma_{MM\text{-}CK}$) and transformed Gibbs free energy of the CK reaction ($\Delta G'_{MM\text{-}CK}$)

A 42% reduction in the $\Gamma_{MM\text{-}CK}$ within creatine-control compared with dextrose-control (Fig. 3B) principally resulted from a 45% increase in PCr (Table 1) and accounted for a gain in $\Delta G'_{MM\text{-}CK}$ of 1.36 kJ/mol. Whereas CLFS induced a decrease in PCr content within both the creatine and dextrose conditions, PCr within creatine-CLFS was still 46% greater than in dextrose-CLFS and 16% higher than in unstimulated dextrose controls (Table 1). Preferential PCr accumulation was also principally responsible for a net gain of $\Delta G'_{MM\text{-}CK}$ of 0.73 kJ/mol within creatine-CLFS compared with dextrose-CLFS.

Total muscle ADP content ($[ADP]_{total}$) was not altered by Cr loading or CLFS (Table 1). In contrast, $[ADP]_{total}/[ADP]_{free}$ was elevated by 50% in Cr-loaded muscles compared with dextrose treatment (Fig. 3C; main effect $P < 0.005$). Consequently, the proportion of ADP_{free} was only 1.8 ± 0.12% in Cr-loaded muscles, compared with 3.0 ± 0.39% in dextrose controls. Regression analysis (Fig. 3D) revealed that the IPP increased as an exponential function of PCr, accounting for 71.3% of the variance (eq. 3; $R^2 = 0.713$, $P < 0.0001$, SE (slope) = 11.0822, SE (y_0) = 0.0065 mmol/kg wet weight, n = 48). Increases in the IPP were proportionally greater above the PCr threshold value of 20 mmol/kg wet weight.

$$\frac{[ATP]}{[ADP]_{free}} = 77.7143 \times e^{0.0685 \times [PCr]} \quad (3)$$

Phospho-AMPKα (Thr172)

Elevation of the IPP was independently confirmed in Cr-loaded muscles by quantifying phospho-AMPKα (Thr172) using western blot (Fig. 4). We reasoned that the greater $[ADP]_{free}$ observed in dextrose-control and dextrose-CLFS compared with Cr-loaded muscles (Table 1) would generate proportional increases in 5′-AMP, via AK, thereby increasing the upstream activity of AMPK-kinase (AMPK-K), which could be detected as greater phospho-AMPKα (Thr172) (Hardie et al. 1999). Furthermore, because allosteric activation of upstream AMPK-K by 5′-AMP is antagonized by competitive ATP binding, and [ATP]/[AMP] varies proportionally with $[ATP]/[ADP]_{free}$, we hypothesised that if the observed increase in $[ATP]/[ADP]_{free}$ (i.e., IPP; Fig. 3A) persisted within Cr-loaded muscles in vivo, the resulting decrease in AMP would yield lower AMPK-K activity and proportionally lower phospho-AMPKα (Thr172) (Figs. 4A, 4B). Phospho-AMPKα (Thr172) was 54% and 63% lower in creatine-CLFS than in dextrose-control and dextrose-CLFS ($P < 0.006$), respectively. Phospho-AMPKα (Thr172) was also 58% lower in creatine-CLFS compared with creatine-control.

MyHC isoform content

The method used to quantify MyHC isoforms is shown in Fig. 5A. Compared with the dextrose-control group, the dextrose-CLFS group displayed substantial fast-to-slow MyHC isoform transitions, characterised by respective 2.0- and 2.7-fold increases in MyHC-I (Fig. 5B, $P < 0.03$) and MyHC-IIa (Fig. 5C, $P < 0.05$) and a 30% decrease in MyHC-IIb (Fig. 5E, $P < 0.03$). In contrast, when Cr-loaded muscles were exposed to CLFS (i.e., creatine-CLFS), fast-to-slow MyHC isoform transitions were abolished (Figs. 5A–5E).

MyHC isoform mRNA

To further investigate the effects of increasing the IPP in vivo on the MyHC adaptive response to CLFS, MyHC isoforms were quantified at the mRNA level. Consistent with the fast-to-slow MyHC isoform transitions observed at the protein level (Fig. 5), the dextrose-CLFS group also demonstrated respective 32-fold (Fig. 6A) and 38-fold (Fig. 6B) increases in MyHC-I and MyHC-IIa mRNA expression and a 5-fold (Fig. 6D) decrease in MyHC-IIb mRNA compared with the dextrose-control group ($P < 0.03$, Fig. 6D). In contrast, although creatine-CLFS induced a 5-fold decrease in MyHC-IIb mRNA compared with creatine-control (Fig. 6D), MyHC-I mRNA and MyHC-IIa mRNA expression levels did not differ from those in the creatine-control or dextrose-control groups (Figs. 6A, 6B).

Calcium ATPase and parvalbumin

The western blot methods used to quantify parvalbumin, SERCA1 (fast isoform), and SERCA2 (slow isoform) are shown in Fig. 7A. CLFS induced a significant decrease in parvalbumin within dextrose-CLFS compared with dextrose-control (Fig. 7B). However, CLFS had no effect on parvalbumin content in Cr-loaded TA muscles (Fig. 7B). CLFS induced similar reductions in SERCA1 within dextrose-CLFS and creatine-CLFS (Fig. 7C); SERCA2 content remained unchanged in dextrose-CLFS but was elevated by 30% ($P < 0.03$) in creatine-CLFS (Fig. 7D). Loading controls (α-actinin, β-actin, and desmin) did not differ within rats or between experimental groups (data not shown).

Reference enzyme activities

Maximum activities of the mitochondrial reference enzymes CS and HADH and the glycolytic enzymes PFK, GAPDH, and CK

Fig. 3. (A) The intracellular phosphorylation potential (IPP), expressed as $[ATP]/[ADP]_{free}$; (B) mass action ratio of creatine kinase ($\Gamma_{MM\text{-}CK}$); (C) $[ADP]_{total}/[ADP]_{free}$; and (D) multivariate regression analysis of $[ATP]/[ADP]_{free}$ as a function of [PCr]. *, Creatine-CLFS greater than dextrose-control ($P < 0.05$).

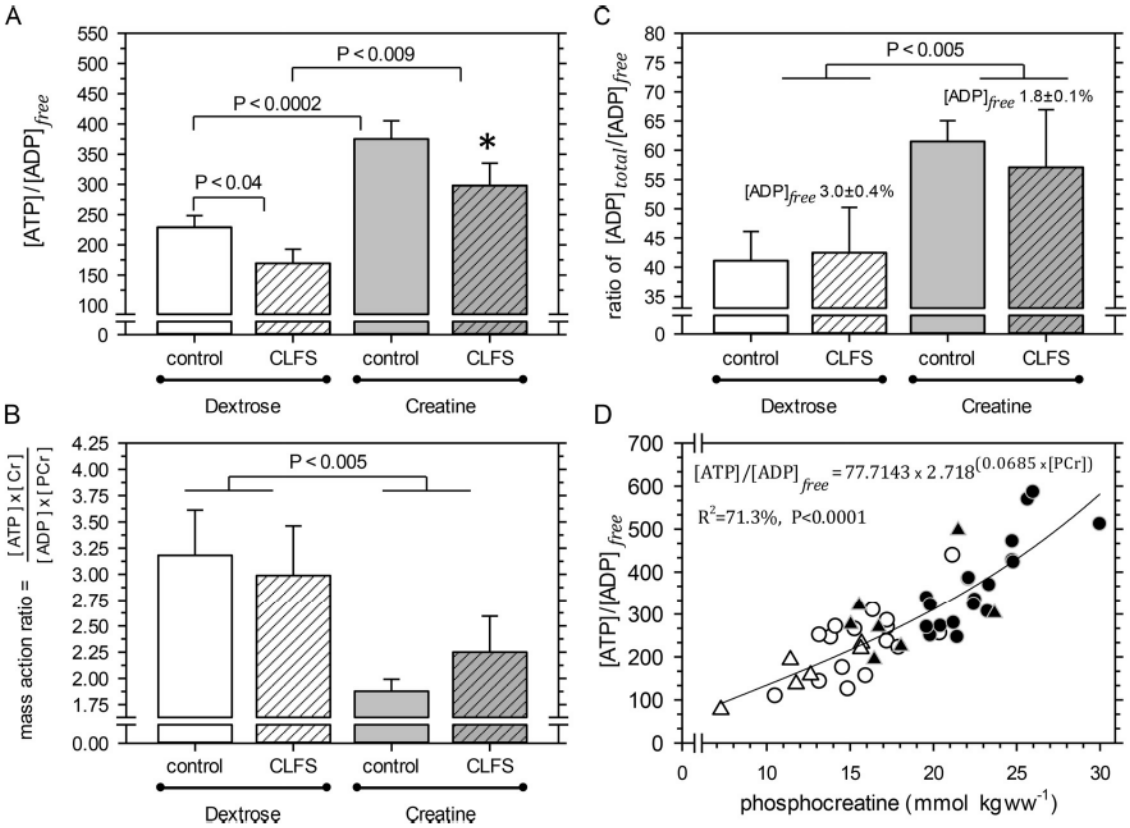

Fig. 4. (A) Representative western blot demonstrating the method used to quantify phospho-AMPKα (Thr172). (B) Relative changes in phospho-AMPKα (Thr172) within tibialis anterior muscles of Sprague–Dawley rats. *, Creatine-CLFS greater than dextrose-control ($P < 0.05$).

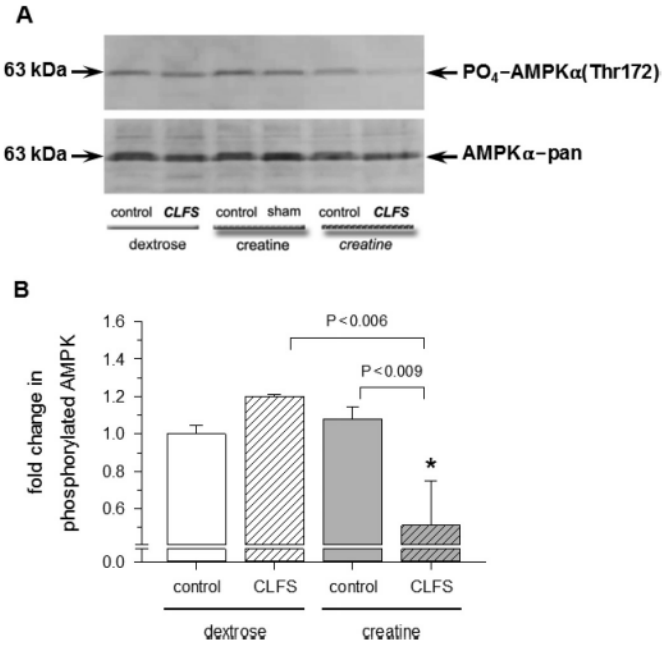

(Table 2) were within the ranges of previous reports (Lowry et al. 1978; Putman et al. 2003, 2004; Gallo et al. 2008). CLFS induced 89% and 34% increases ($P < 0.01$) in the respective maximum activities of CS and HADH in dextrose-CLFS and similar 77% and 58% increases ($P < 0.01$) in creatine-CLFS. CK activities declined to similar levels in dextrose-CLFS and creatine-CLFS ($P < 0.03$). In contrast, whereas CLFS induced ~22% reductions in PFK ($P < 0.01$) and GAPDH ($P < 0.02$) within dextrose-CLFS, PFK ($P > 0.94$) and GAPDH ($P > 0.51$) activities remained unchanged in creatine-CLFS.

Isometric functional measures

Measures of isometric muscle power output (TW_f) and contractile speed (TTP, ½RT, ½FT) are summarised in Table 3. Neither the Cr-loading nor CLFS treatments alone had any significant effects on TW_f. Cr loading did, however, prolong the TTP by ~7.6 ms (~20%, main effect $P < 0.01$) and the ½RT by ~2.6 ms (~22%, main effect $P < 0.001$).

Discussion

This study is the first to investigate whether increasing the IPP in rat fast-twitch TA muscle can prevent CLFS-induced fast-to-slow transitions. Twenty days of Cr feeding proved to be a successful experimental model to increase TCr, PCr, and the IPP. Furthermore, the application of CLFS to Cr-loaded TA muscles on days 11–20 proved to be a very good experimental model in which to investigate activity-induced fibre type transitions in the presence of an increased IPP. The novel findings of this study are that chronic elevation of the IPP in rat fast-twitch muscles significantly changed the adaptive response to 10 days of CLFS by (*i*) abolishing fast-to-slow MyHC transitions, (*ii*) preventing a reduction in glycolytic potential but not at the expense of an

Fig. 5. (A) Method used to quantify the MyHC isoform content in tibialis anterior muscles of Sprague–Dawley rats. Relative change in (B) MyHC-I, (C) MyHC-IIa, (D) MyHC-IId/x, and (E) MyHC-IIb.

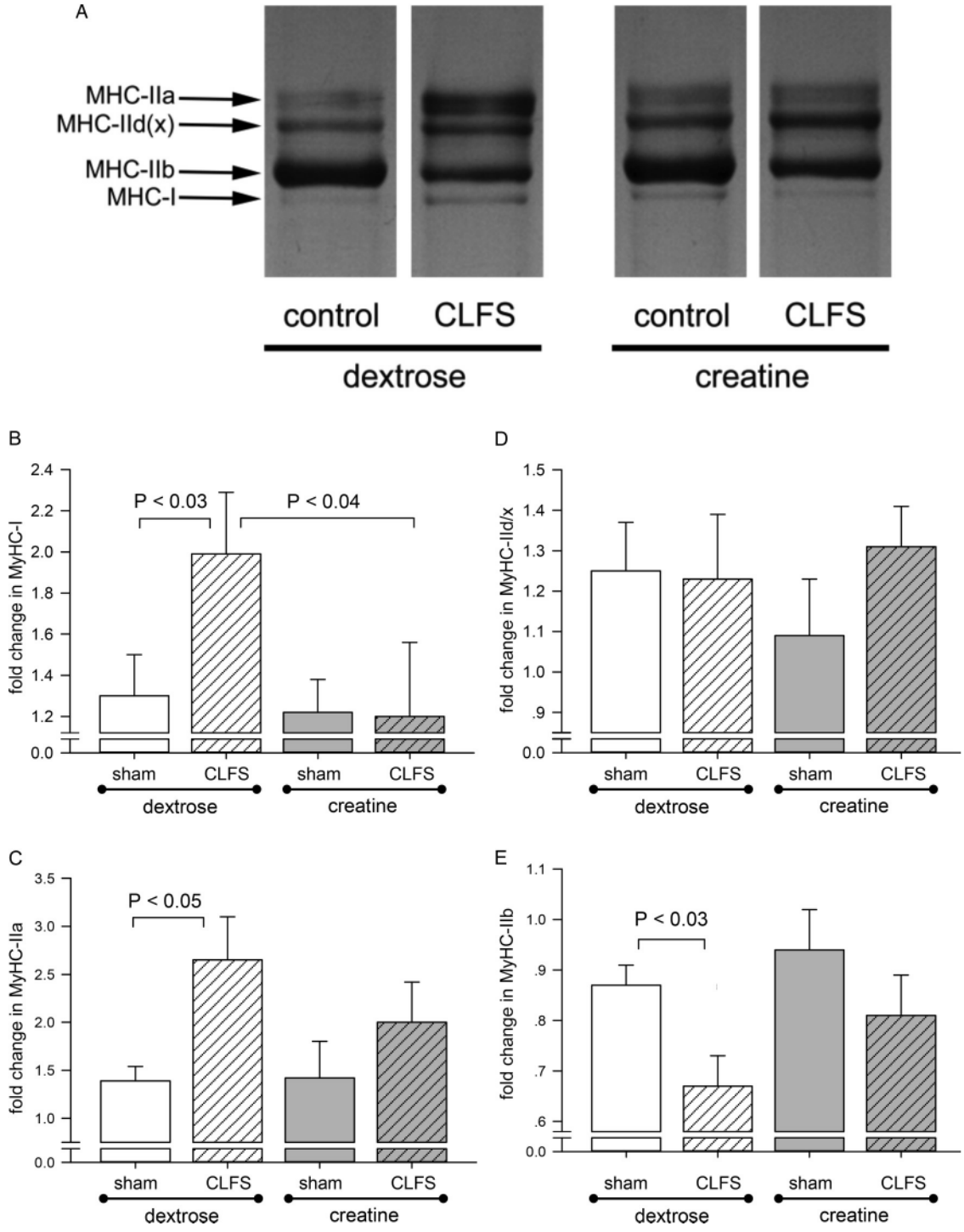

increase in muscle oxidative capacity, (*iii*) abolishing decreases in parvalbumin content, and (*iv*) further increasing total SERCA content.

Cr loading increases PCr accretion and the IPP

The preferential increase in PCr (i.e., 7.0 mmol/kg wet weight) observed in the present study accounted for 74% of the increase in TCr (i.e., 9.5 mmol/kg wet weight), which appears to be in agreement with the findings of McMillen et al. (2001). They reported that an increase in PCr of 3.0 mmol/kg wet weight accounted for 68% of the increase in TCr, but they did not detect a change in the IPP. This appears to be because the maximum PCr value they reported was <20 mmol/kg wet weight. In contrast, the 2.3-fold greater increase in PCr that occurred in our study included values >20 mmol/kg wet weight, which is the threshold at which the IPP begins to increase exponentially as a function of increasing PCr (Fig. 3D). Our observations are consistent with the rodent single-fibre studies of Conjard et al. (1998), who demonstrated the same relationship within the same critical range of 20–33 mmol/kg wet weight (i.e., 85–140 mmol/kg dry weight).

Fig. 6. Changes in MyHC mRNA expression for (A) MyHC-I, (B) MyHC-IIa, (C) MyHC-IId/x, and (D) MyHC-IIb.

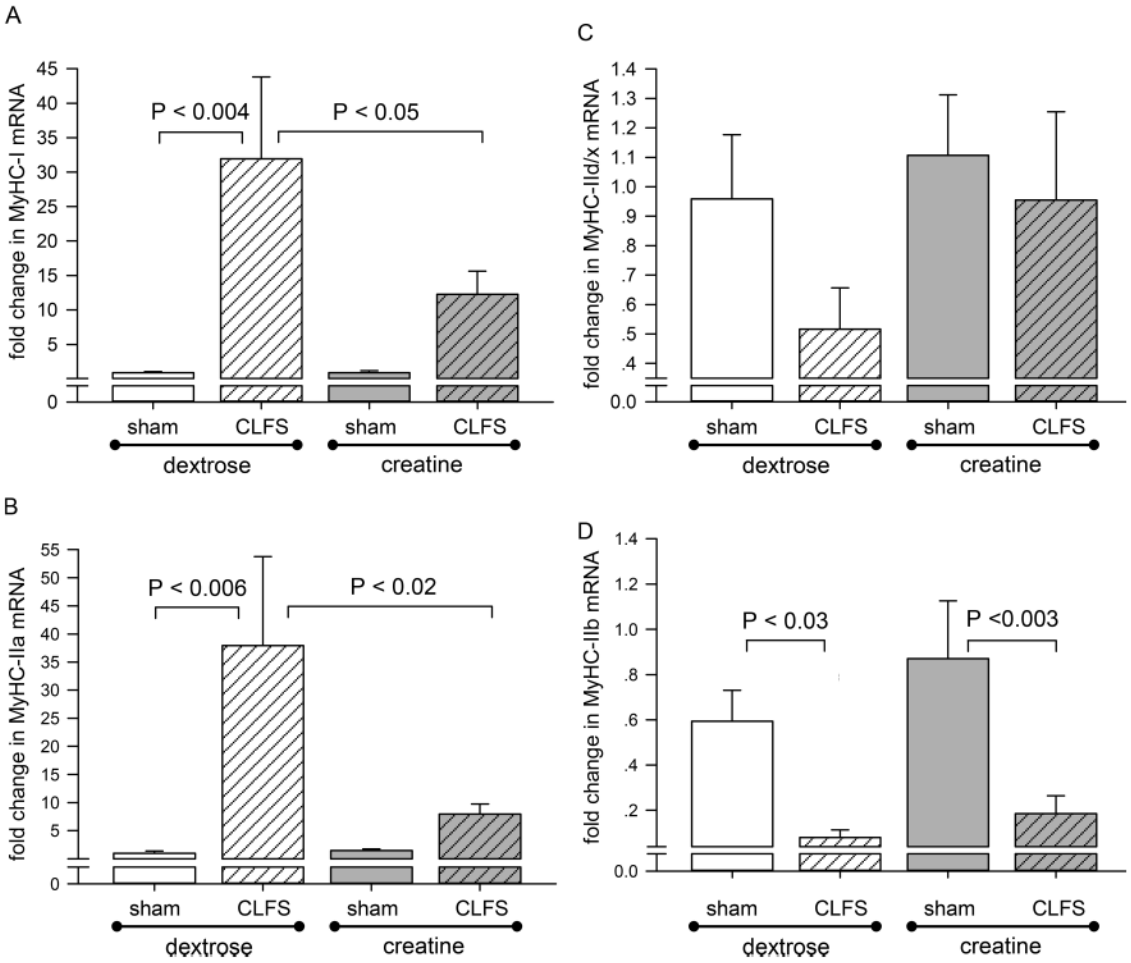

The creatine-induced increase in the IPP appears to have resulted from the integration of 3 intracellular systems. (*i*) Sequential reactions catalysed by the near-equilibrium enzymes CK ($Cr^0 + ATP^{4-} \rightarrow PCr^{2-} + ADP^{3-} + H^+$) and AK ($2ADP^{3-} \rightarrow ATP^{4-} + AMP^{2-}$) (Golding et al. 1995; Nabuurs et al. 2010) should have ensured removal of cytosolic ADP_{free}; further reductions in available ADP_{free} (Fig. 3C) most likely resulted from low-affinity binding of ADP to soluble proteins, which is known to increase in response to training (Sahlin and Harris 2011). (*ii*) Likewise, the CK-generated H^+ most certainly was removed or "buffered" according to the physiochemical principles that govern acid-base balance in muscle (Lindinger et al. 2005). (*iii*) Finally, a 41% increase in the PCr/ATP ratio without corresponding increases in Cr and ATP could have occurred only if the larger PCr pool was accommodated by an increase in intracellular binding to low-affinity sites, such as zwitterionic phospholipids (Tokarska-Schlattner et al. 2012).

Thermodynamic consequences of Cr loading on the CK system

Preferential PCr accumulation (Table 1) was principally responsible for a ~35% decrease in the $\Gamma_{MM\text{-}CK}$ relative to the $K'_{eq\ MM\text{-}CK}$ in the creatine-control group (Fig. 3B) and a ~25% decrease in the creatine-CLFS group (Fig. 3B). The respective 13% and 7% gains in $\Delta G'_{MM\text{-}CK}$ should have enhanced the functional capacity and kinetic properties of the CK system as a spatial and temporal energy buffer of ATP (Wallimann et al. 1992; Aliev et al. 2011). Furthermore, because ADP_{free} is only transiently available in vivo (Nabuurs et al. 2010) and the magnitude of spikes in ADP_{free} is inversely proportional to [PCr] (Sahlin and Harris 2011), these calculated gains in $\Delta G'_{MM\text{-}CK}$ must be considered minimum values. Thus it would seem that the major benefit derived from a more uniform distribution of a higher IPP relates to an increase in thermodynamic efficiency of ATP hydrolysis within muscle fibres (Wallimann et al. 1992).

MyHC fibre type transitions

As an experimental model of muscle training, CLFS has proven indispensable in revealing the adaptive potential of muscle fibres and providing important temporal clues to the physiological signals and molecular events that determine postnatal fibre remodelling (Pette and Vrbová 1999). In the present study, CLFS-induced fast-to-slow MyHC isoform transitions, at the protein (Fig. 5) and mRNA (Fig. 6) levels, were similar to those previously reported (Putman et al. 2003, 2004; Martins et al. 2012). Compared with voluntary running, which was used in our previous study (Gallo et al. 2008) to investigate fast-to-slow fibre type transitions within plantaris of the same rat strain, CLFS induced more advanced fibre type conversion over a much shorter time period and proved to be a better experimental model. In our previous study, 91 days of Cr feeding induced a 20% increase in TCr, which was sufficient to attenuate but not abolish running-induced fast-to-slow MyHC fibre type transitions in the plantaris (Gallo et al. 2006, 2008). In the present study, however, a 34% increase in TCr elevated the IPP within TA muscles and abolished CLFS-induced fast-to-slow MyHC isoform transitions (Figs. 5 and 6).

Our findings point to the interesting possibility that MyHC-I, MyHC-IIa, and MyHC-IIb expression levels are transcriptionally

Fig. 7. (A) Representative immunoblots of parvalbumin, SERCA1, and SERCA2 in tibialis anterior muscles of Sprague–Dawley rats. Changes in the contents of (B) parvalbumin, (C) SERCA1, and (D) SERCA2.

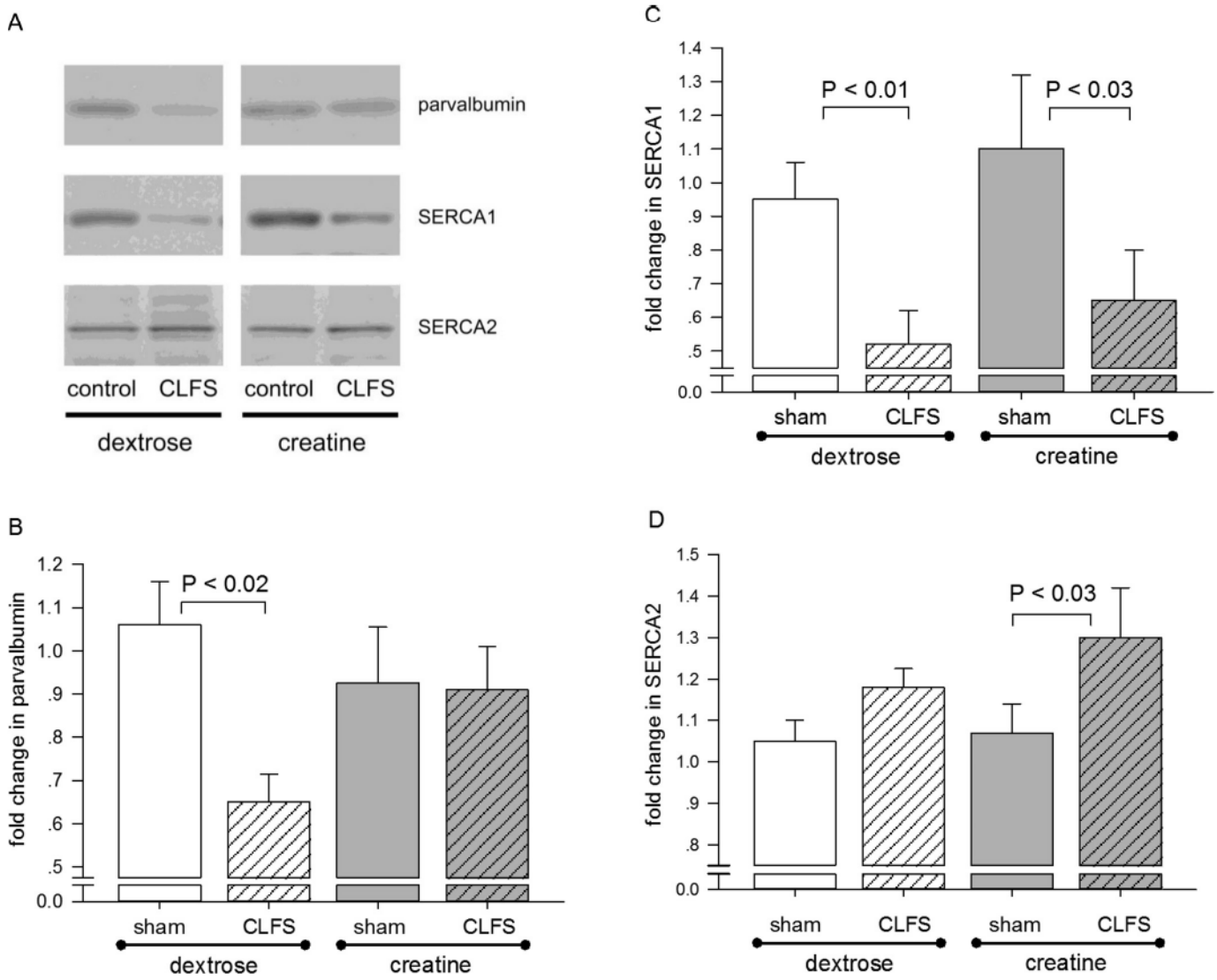

Table 2. Maximum activities of citrate synthase (CS, EC 2.3.3.1), 3-hydroxyacyl-CoA dehydrogenase (HADH, EC 1.1.1.35), phosphofructokinase (PFK, EC 2.7.1.11), glyceraldehyde-3-phosphate dehydrogenase (GAPDH, EC 1.2.1.12), and creatine kinase (CK, EC 2.7.3.2) in tibialis anterior muscles of Sprague–Dawley rats.

Treatment	Muscle	CS	HADH	PFK	GAPDH	CK
Dextrose	Contralateral control	35.9±3.4	11.6±0.7	23.1±4.4	507±33	3927±91
	Sham	40.6±1.6	14.5±1.5	22.2±2.7	485±37	3587±138
Dextrose	Contralateral control	29.3±2.9	11.9±0.6	29.4±4.3	464±26	3745±184
	CLFS	55.5±3.1*	16.0±1.9*	22.8±4.0*	364±35*	3160±215*
Creatine	Contralateral control	26.6±3.2	10.9±0.8	26.9±3.2	464±38	4120±233
	Sham	37.0±3.9	13.9±1.2	34.4±3.5	452±31	3718±104
Creatine	Contralateral control	26.7±2.5	10.4±0.8	19.4±2.6	492±40	3830±84
	CLFS	47.3±3.5*	16.4±1.4*	19.2±2.8	469±39	2881±184*

Note: Data are means ± SE. Enzyme activities are expressed as units (i.e., 1 μmol/min at 30 °C) per gram of wet muscle weight.
*Chronic low-frequency stimulation (CLFS) different from contralateral control ($P < 0.01$).

regulated by an energy-sensitive response element. Whether such regulation is direct or is part of an integrated, universal signal remains an intriguing question. In this regard, it is interesting to consider the relationship between the IPP and intracellular [Ca^{2+}]. During contractions, SERCA activity is dependent on the maintenance of high local IPP and is inversely proportional to cytoplasmic [Ca^{2+}] (Pulido et al. 1998; Duke and Steele 1999). The application of CLFS for a time period similar to that used in the present study has been shown to lower PCr, lower the IPP (Conjard et al. 1998), and induce 2-fold increases in resting intracellular [Ca^{2+}] (e.g., 0.75 to 1.6 μmol/L) and integral [Ca^{2+}] per stimulation pulse (Carroll et al. 1999). Thus, increases in PCr and IPP coupled with higher parvalbumin content in creatine-CLFS should have increased the rate of ATP-dependent Ca^{2+} re-uptake by SERCAs

Table 3. Isometric functional measures of tibialis anterior muscles of Sprague–Dawley rats.

Treatment	Muscle	TW_f (mN)	TTP† (ms)	½RT† (ms)	½FT (ms)
Dextrose	Contralateral control	2855±126	39.0±1.2	11.6±0.2	42.5±1.7
	Sham	2445±270	38.0±1.4	11.9±0.6	31.0±2.9
Dextrose	Contralateral control	3119±339	43.9±3.8	12.8±0.7	44.8±3.4
	CLFS	2694±278	47.8±3.1	14.0±0.6*	43.1±4.6
Creatine	Contralateral control	3323±182	44.5±1.5	14.1±0.5	45.2±4.3
	Sham	2857±218	47.7±1.8	14.5±0.5	41.6±2.9
Creatine	Contralateral control	3188±125	50.4±1.6	14.8±0.4	48.3±3.9
	CLFS	2409±135	51.4±2.4	15.4±0.6	46.0±4.0

Note: Data are means ± SE. TW_f, isometric twitch force; TTP, time to peak tension; ½RT, half-rise time; ½FT, half-fall time.

*Chronic low-frequency stimulation (CLFS) different from contralateral control ($P < 0.01$).

†Creatine loading resulted in prolonged TTP and 1/2RT (main effect of creatine treatment, $P < 0.01$).

and reduced Ca^{2+} signalling. We propose that under those prevailing intracellular conditions, more efficient intracellular Ca^{2+} channelling within Ca^{2+} nanodomains (Rossi et al. 2011) formed the basis for lower resting intracellular [Ca^{2+}] and integral [Ca^{2+}] per stimulation. Indeed, such a hypothesis is consistent with the reduction in intracellular [Ca^{2+}] by Cr in vitro (Pulido et al. 1998) and the severely reduced calcineurin activity in transgenic mice that overexpress parvalbumin (Chin et al. 2003).

Because expression of the predominant MyHC-IIb isoform remained unchanged in creatine-CLFS, despite a 75% decrease in mRNA (Figs. 5 and 6), it is reasonable to conclude that transcriptional regulation of MyHC-IIb was overridden in our experimental model by post-translational processes. Thus it is interesting to consider that the substantially lower rate of MyHC-IIb protein turnover that must have occurred in creatine-CLFS was associated with the neutralisation of peroxynitrite ($OONO^-$) by Cr (Lawler et al. 2002) and $OONO^-$-dependent inactivation of the ubiquitin proteolytic pathway (Rabuel et al. 2010). Indeed, Klebl et al. (1998) showed that CLFS induced considerable $OONO^-$-mediated S-nitrosylation of amino acid residues, and Moriscot et al. (2010) reported that the ubiquitin ligases MAFbx and MuRF1 are preferentially expressed within type II fibres. It is also possible that lower resting intracellular [Ca^{2+}] provided an extra measure of protection against Ca^{2+}-activated calpain-mediated proteolysis of MyHC-IIb (Sultan et al. 2000).

Calcium regulatory proteins and isometric muscle function

Several studies have demonstrated that the rates of muscle contraction and relaxation are positively correlated with parvalbumin levels (Huber and Pette 1996; Carroll et al. 1999; Chin et al. 2003) and that parvalbumin content is typically reduced by ~50% within just 6 to 14 days of CLFS (Huber and Pette 1996; Carroll et al. 1999). A comparable reduction in parvalbumin (Fig. 7) and a slower rate of force development occurred within the dextrose-CLFS group in our study, as reflected by a 19% increase in the ½RT (Table 3). However, this did not occur in Cr-loaded muscles exposed to CLFS. Because Cr-loaded muscles retained high levels of parvalbumin after 10 days of CLFS that were similar to those in unstimulated dextrose controls, we expected comparably fast contraction parameters. In the present study, however, longer TTP and ½RT in Cr-loaded muscles appeared to form the basis for improved contractile function, which emphasised a greater capacity to generate and sustain force output, such as maximum tetanic force production (TET_f). This finding is consistent with our previous study in which 91 days of Cr loading of rat plantaris increased TET_f and improved fatigue resistance, as reflected in lower fatigue indexes at 10 and 30 s (Gallo et al. 2006). Thus it would seem that the improved contractile function of Cr-loaded muscles results from retaining an abundance of larger fast fibres with improved fatigue resistance.

Metabolic profile

The CLFS-induced changes in glycolytic (i.e., GAPDH and PFK) and oxidative (i.e., CS and HADH) capacities observed in dextrose-CLFS were similar in magnitude to those observed in previous studies from our lab (Putman et al. 2003, 2004, 2007) and others (for reviews see Pette and Staron 1997; Pette and Vrbová 1999) during a well-characterised phase of rapid fast-to-slow fibre type transitions. Abolishment of CLFS-induced reductions in the glycolytic reference enzymes PFK and GAPDH in creatine-CLFS suggests that regulatory events that are sensitive to fluctuations in the IPP may also exert control over the expression of PFK and GAPDH. Although it is known that expression of glycolytic and oxidative reference enzymes is regulated by transcriptional, translational, and post-translational events, it remains to be determined which of these events were influenced by the elevated IPP within our experimental model. IPP-dependent variations in myogenin expression levels (Hughes et al. 1999) and calcineurin activity (Meissner et al. 2001) remain interesting possibilities.

Based on the studies of Ingwall (1976), we hypothesised that maximum CK activity would increase after a period of prolonged exposure to higher concentrations of intramuscular Cr and provide an additional measure of protection against CLFS-induced decreases in CK. However, this did not occur. Cr loading did not influence CK activity, nor did it prevent a 33% decrease in CK activity in creatine-CLFS (Table 2). The present data do not, however, distinguish between cytosolic CK (MM-CK) and mitochondrial CK (Mi-CK) isoforms. In light of the significant increases in mitochondrial reference enzymes, it is reasonable to expect that a proportional shift from MM-CK toward Mi-CK would have occurred, resulting in an increased capacity for PCr production without altering the capacity of the CK system (Aliev et al. 2011).

Potential pleiotropic effects of creatine

Current theories attempting to explain how Cr loading influences muscle gene expression have focussed only on putative pleiotropic effects of Cr and have ignored the potential of the IPP to transduce contraction-dependent signalling (Wallimann et al. 2011). However, 3 lines of evidence argue against the involvement of pleiotropic Cr effects in our study. First, hyperosmolarity did not occur in the present study or in our previous studies (Gallo et al. 2006, 2008). Second, β-GPA does not induce expression of "osmosensing" genes, even though it has a higher affinity for cellular uptake, accumulates as phosphorylated β-GPA, and has the potential to generate greater increases in osmolarity (Oudman et al. 2013). Third, if Cr possessed the potential to directly regulate the expression of other gene families, then it follows that β-GPA should exert the same effect, but it does not. In fact, administration of β-GPA is known to have the opposite effect on muscle gene expression (Ren et al. 1995; Brault et al. 2003). It is therefore more plausible that the fundamentally divergent cellular effects of

β-GPA and Cr on muscle gene expression are a function of the opposite effects they exert on the IPP.

Conclusion and knowledge translation

This study is the first to show that when mixed fast-twitch muscles are Cr-loaded before and during prolonged exposure to an endurance-training stimulus, they maintain a fast-twitch glycolytic phenotype but also adapt to the training stimulus by increasing oxidative capacity. Thus the IPP would seem to play an important role in determining the adaptive response of skeletal muscle fibres to a chronic training stimulus that encompasses improvements in both muscular endurance and muscular power that are not mutually exclusive. The findings of this study are particularly relevant to human inherited neuromuscular pathologies such as amyotrophic lateral sclerosis, spinal muscular atrophy, and muscular dystrophies that typically include chronic cycles of muscle fibre inflammation, degeneration, and regeneration, particularly within fast fibre populations. Under these circumstances, muscle creatine depletion develops secondary to the primary lesion but nevertheless contributes to pathogenesis. In light of the ability of PCr and Cr to weakly bind to zwitterionic phospholipids and protect membrane permeability (Tokarska-Schlattner et al. 2012), oral creatine supplementation should prove to be a beneficial adjunct therapy to quickly replenish muscle PCr and Cr stores, restore the IPP, and enhance cell signalling.

Acknowledgements

This study was funded by grants from the Natural Sciences and Engineering Research Council (NSERC) of Canada to C.T.P. and W.T.D. and from Alberta Innovates–Health Solutions (AIHS) to C.T.P. and T.G. The authors thank Y. Shu and N. Tyreman for completing animal experiments and Z. Kenwell for constructing CLFS stimulation units. M.G. was supported by Izaak Walton Killam and NSERC PGS-D scholarships. K.J.B.M. was supported by AIHS and NSERC PGS-D scholarships. M.J.J. was supported by consecutive USRA, PGS-M, and CGS-D NSERC scholarships. C.T.P. is a Senior Scholar of AIHS.

References

Aliev, M., Guzun, R., Karu-Varikmaa, M., Kaambre, T., Wallimann, T., and Saks, V. 2011. Molecular system bioenergics of the heart: experimental studies of metabolic compartmentation and energy fluxes versus computer modeling. Int. J. Mol. Sci. 12(12): 9296–9331. doi:10.3390/ijms12129296. PMID:22272134.

Brault, J.J., Abraham, K.A., and Terjung, R.L. 2003. Muscle creatine uptake and creatine transporter expression in response to creatine supplementation and depletion. J. Appl. Physiol. 94(6): 2173–2180. doi:10.1063/1.1591071, 10.1152/japplphysiol.01171.2002. PMID:12611762.

Carroll, S.L., Nicotera, P., and Pette, D. 1999. Calcium transients in single fibers of low-frequency stimulated fast-twitch muscle of rat. Am. J. Physiol. Cell Physiol. 277(6): C1122–C1129. PMID:10600763.

Chin, E.R., Grange, R.W., Viau, F., Simard, A.R., Humphries, C., Shelton, J., et al. 2003. Alterations in slow-twitch muscle phenotype in transgenic mice overexpressing the Ca^{2+} buffering protein parvalbumin. J. Physiol. 547(2): 649–663. doi:10.1113/jphysiol.2002.024760. PMID:12562945.

Cieslar, J.H., and Dobson, G.P. 2000. Free [ADP] and aerobic muscle work follow at least second order kinetics in rat gastrocnemius in vivo. J. Biol. Chem. 275(9): 6129–6134. doi:10.1074/jbc.275.9.6129. PMID:10692403.

Cieslar, J., Huang, M.T., and Dobson, G.P. 1998. Tissue spaces in rat heart, liver, and skeletal muscle in vivo. Am. J. Physiol. Regul. Integr. Comp. Physiol. 275(5): R1530–R1536. PMID:9791070.

Conjard, A., Peuker, H., and Pette, D. 1998. Energy state and myosin heavy chain isoforms in single fibres of normal and transforming rabbit muscles. Pflügers Arch. 436(6): 962–969. doi:10.1007/s004240050730. PMID:9799414.

Duke, A.M., and Steele, D.S. 1999. Effects of creatine phosphate on Ca^{2+} regulation by the sarcoplasmic reticulum in mechanically skinned rat skeletal muscle fibres. J. Physiol. 517(2): 447–458. doi:10.1111/j.1469-7793.1999.0447t.x. PMID:10332094.

Gallo, M., Gordon, T., Syrotuik, D., Shu, Y., Tyreman, N., Maclean, I., et al. 2006. Effects of long-term creatine feeding and running on isometric functional measures and myosin heavy chain content of rat skeletal muscles. Pflügers Arch. 452(6): 744–755. doi:10.1007/s00424-006-0079-0. PMID:16688465.

Gallo, M., Maclean, I., Tyreman, N., Martins, K.J., Syrotuik, D., Gordon, T., and Putman, C.T. 2008. Adaptive responses to creatine loading and exercise in fast-twitch rat skeletal muscle. Am. J. Physiol. Regul. Integr. Comp. Physiol. 294(4): R1319–R1328. doi:10.1152/ajpregu.00631.2007. PMID:18216140.

Golding, E.M., Teague, W.E., Jr., and Dobson, G.P. 1995. Adjustment of K′ to varying pH and pMg for the creatine kinase, adenylate kinase and ATP hydrolysis equilibria permitting quantitative bioenergetic assessment. J. Exp. Biol. 198(8): 1775–1782. PMID:7636446.

Green, H.J., and Pette, D. 1997. Early metabolic adaptations of rabbit fast-twitch muscle to chronic low-frequency stimulation. Eur. J. Appl. Physiol. Occup. Physiol. 75(5): 418–424. doi:10.1007/s004210050182. PMID:9189729.

Green, H.J., Düsterhöft, S., Dux, L., and Pette, D. 1992. Metabolite patterns related to exhaustion, recovery and transformation of chronically stimulated rabbit fast-twitch muscle. Pflügers Arch. 420(3–4): 359–366. doi:10.1007/BF00374471. PMID:1598191.

Hämäläinen, N., and Pette, D. 1997. Coordinated fast-to-slow transitions of myosin and SERCA isoforms in chronically stimulated muscles of euthyroid and hyperthyroid rabbits. J. Muscle Res. Cell Motil. 18(5): 545–554. doi:10.1023/A:1018663218477. PMID:9350007.

Hämäläinen, N., and Pette, D. 2001. Myosin and SERCA isoform expression in denervated slow-twitch muscle of euthyroid and hyperthyroid rabbits. J. Muscle Res. Cell Motil. 22(5): 453–457. doi:10.1023/A:1014543507149. PMID:11964070.

Hardie, D.G., Salt, I.P., Hawley, S.A., and Davies, S.P. 1999. AMP-activated protein kinase: an ultrasensitive system for monitoring cellular energy charge. Biochem. J. 338(3): 717–722. doi:10.1042/0264-6021:3380717. PMID:10051444.

Harris, R.C., Soderlund, K., and Hultman, E. 1992. Elevation of creatine in resting and exercised muscle of normal subjects by creatine supplementation. Clin. Sci. 83: 367–374. PMID:1327657.

Henriksson, J., Salmons, S., Chi, M.Y., Hintz, C.S., and Lowry, O.H. 1988. Chronic stimulation of mammalian muscle: changes in metabolite concentrations in individual fibers. Am. J. Physiol Cell Physiol. 255(4): C543–C551. PMID:3177628.

Huber, B., and Pette, D. 1996. Dynamics of parvalbumin expression in low-frequency-stimulated fast-twitch rat muscle. Eur. J. Biochem. 236(3): 814–819. doi:10.1111/j.1432-1033.1996.t01-2-00814.x. PMID:8665899.

Hughes, S.M., Chi, M.M., Lowry, O.H., and Gundersen, K. 1999. Myogenin induces a shift of enzyme activity from glycolytic to oxidative metabolism in muscles of transgenic mice. J. Cell Biol. 145(3): 633–642. doi:10.1083/jcb.145.3.633. PMID:10225962.

Ingwall, J.S. 1976. Creatine and the control of muscle-specific protein synthesis in cardiac and skeletal muscle. Circ. Res. 38(5 Suppl. 1): I-115–I-123. PMID:1269086.

Klebl, B.M., Ayoub, A.T., and Pette, D. 1998. Protein oxidation, tyrosine nitration, and inactivation of sarcoplasmic reticulum Ca^{2+}-ATPase in low-frequency stimulated rabbit muscle. FEBS Lett. 422(3): 381–384. doi:10.1016/S0014-5793(98)00053-2. PMID:9498821.

Lawler, J.M., Barnes, W.S., Wu, G., Song, W., and Demaree, S. 2002. Direct antioxidant properties of creatine. Biochem. Biophys. Res. Commun. 290(1): 47–52. doi:10.1006/bbrc.2001.6164. PMID:11779131.

Lindinger, M.I., Kowalchuk, J.M., and Heigenhauser, G.J. 2005. Applying physicochemical principles to skeletal muscle acid-base status. Am. J. Physiol. Regul. Integr. Comp. Physiol. 289(3): R891–R894. doi:10.1152/ajpregu.00225.2005. PMID:16105823.

Lowry, C.V., Kimmey, J.S., Felder, S., Chi, M.M., Kaiser, K.K., Passonneau, P.N., et al. 1978. Enzyme patterns in single human muscle fibers. J. Biol. Chem. 253(22): 8269–8277. PMID:152314.

Martins, K.J., St-Louis, M., Murdoch, G.K., MacLean, I.M., McDonald, P., Dixon, W.T., et al. 2012. Nitric oxide synthase inhibition prevents activity-induced calcineurin-NFATc1 signalling and fast-to-slow skeletal muscle fibre type conversions. J. Physiol. 590(6): 1427–1442. doi:10.1113/jphysiol.2011.223370. PMID:22219342.

McMillen, J., Donovan, C.M., Messer, J.I., and Willis, W.T. 2001. Energetic driving forces are maintained in resting rat skeletal muscle after dietary creatine supplementation. J. Appl. Physiol. 90(1): 62–66. PMID:11133894.

Meissner, J.D., Gros, G., Scheibe, R.J., Scholz, M., and Kubis, H.P. 2001. Calcineurin regulates slow myosin, but not fast myosin or metabolic enzymes, during fast-to-slow transformation in rabbit skeletal muscle cell culture. J. Physiol. 533(1): 215–226. doi:10.1111/j.1469-7793.2001.0215b.x. PMID:11351029.

Moriscot, A.S., Baptista, I.L., Bogomolovas, J., Witt, C., Hirner, S., Granzier, H., and Labeit, S. 2010. MuRF1 is a muscle fiber-type II associated factor and together with MuRF2 regulates type-II fiber trophicity and maintenance. J. Struct. Biol. 170(2): 344–353. doi:10.1016/j.jsb.2010.02.001. PMID:20149877.

Nabuurs, C., Huijbregts, B., Wieringa, B., Hilbers, C.W., and Heerschap, A. 2010. 31P saturation transfer spectroscopy predicts differential intracellular macromolecular association of ATP and ADP in skeletal muscle. J. Biol. Chem. 285(51): 39588–39596. doi:10.1074/jbc.M110.164665. PMID:20884612.

Newsholme, E.A., and Crabtree, B. 1979. Theoretical principles in the approaches to control of metabolic pathways and their application to glycolysis in muscle. J. Mol. Cell. Cardiol. 11(9): 839–856. doi:10.1016/0022-2828(79)90480-2. PMID:490659.

Newsholme, E.A., Beis, I., Leech, A.R., and Zammit, V.A. 1978. The role of creatine kinase and arginine kinase in muscle. Biochem. J. 172: 533–537. PMID:210761.

Oudman, I., Clark, J.F., and Brewster, L.M. 2013. The effect of the creatine analogue beta-guanidinopropionic acid on energy metabolism: a systematic

review. PLoS One, 8(1): e52879. doi:10.1371/journal.pone.0052879. PMID: 23326362.

Pette, D., and Staron, R.S. 1997. Mammalian skeletal muscle fiber type transitions. Int. Rev. Cytol. 170: 143–223. doi:10.1016/S0074-7696(08)61622-8. PMID: 9002237.

Pette, D., and Vrbová, G. 1999. What does chronic electrical stimulation teach us about muscle plasticity? Muscle Nerve, 22(6): 666–677. doi:10.1002/(SICI)1097-4598(199906)22:6<666::AID-MUS3>3.0.CO;2-Z. PMID:10366220.

Pulido, S.M., Passaquin, A.C., Leijendekker, W.J., Challet, C., Wallimann, T., and Ruegg, U.T. 1998. Creatine supplementation improves intracellular Ca^{2+} handling and survival in mdx skeletal muscle cells. FEBS Lett. 439(3): 357–362. doi:10.1016/S0014-5793(98)01399-4. PMID:9845353.

Putman, C.T., Jones, N.L., Hultman, E., Hollidge-Horvat, M.G., Bonen, A., McConachie, D.R., and Heigenhauser, G.J. 1998. Effects of short-term submaximal training in humans on muscle metabolism in exercise. Am. J. Physiol. Endocrinol. Metab. 275(1): E132–E139. PMID:9688884.

Putman, C.T., Kiricsi, M., Pearcey, J., MacLean, I.M., Bamford, J.A., Murdoch, G.K., et al. 2003. AMPK activation increases uncoupling protein-3 expression and mitochondrial enzyme activities in rat muscle without fibre type transitions. J. Physiol. 551(1): 169–178. doi:10.1113/jphysiol.2003.040691. PMID:12813156.

Putman, C.T., Dixon, W.T., Pearcey, J., MacLean, I.M., Jendral, M.J., Kiricsi, M., et al. 2004. Chronic low-frequency stimulation up-regulates uncoupling protein-3 in transforming rat fast-twitch skeletal muscle. Am. J. Physiol. Regul. Integr. Comp. Physiol. 287(6): R1419–R1426. doi:10.1152/ajpregu.00421.2004. PMID:15308491.

Putman, C.T., Martins, K.J., Gallo, M.E., Lopaschuk, G.D., Pearcey, J.A., MacLean, I.M., et al. 2007. Alpha-catalytic subunits of 5′AMP-activated protein kinase display fiber-specific expression and are upregulated by chronic low-frequency stimulation in rat muscle. Am. J. Physiol. Regul. Integr. Comp. Physiol. 293(3): R1325–R1334. doi:10.1152/ajpregu.00609.2006. PMID:17553841.

Rabuel, C., Samuel, J.L., Lortat-Jacob, B., Marotte, F., Lanone, S., Keyser, C., et al. 2010. Activation of the ubiquitin proteolytic pathway in human septic heart and diaphragm. Cardiovasc. Pathol. 19(3): 158–164. doi:10.1016/j.carpath.2009.01.002. PMID:19375358.

Ren, J.M., Ohira, Y., Holloszy, J.O., Hämäläinen, N., Traub, I., and Pette, D. 1995. Effects of beta-guanidinopropionic acid-feeding on the patterns of myosin isoforms in rat fast-twitch muscle. Pflügers Arch. 430(3): 389–393. doi:10.1007/BF00373914. PMID:7491263.

Rossi, A.E., Boncompagni, S., Wei, L., Protasi, F., and Dirksen, R.T. 2011. Differential impact of mitochondrial positioning on mitochondrial Ca^{2+} uptake and Ca^{2+} spark suppression in skeletal muscle. Am. J. Physiol Cell Physiol. 301(5): C1128–C1139. doi:10.1152/ajpcell.00194.2011. PMID:21849670.

Roussel, D., Lhenry, F., Ecochard, L., Sempore, B., Rouanet, J.L., and Favier, R. 2000. Differential effects of endurance training and creatine depletion on regional mitochondrial adaptations in rat skeletal muscle. Biochem. J. 350(2): 547–553. doi:10.1042/0264-6021:3500547. PMID:10947970.

Sahlin, K., and Harris, R.C. 2011. The creatine kinase reaction: a simple reaction with functional complexity. Amino Acids, 40(5): 1363–1367. doi:10.1007/s00726-011-0856-8. PMID:21394603.

Snow, R.J., and Murphy, R.M. 2003. Factors influencing creatine loading into human skeletal muscle. Exerc. Sport Sci. Rev. 31(3): 154–158. doi:10.1097/00003677-200307000-00010. PMID:12882483.

Sultan, K.R., Dittrich, B.T., and Pette, D. 2000. Calpain activity in fast, slow, transforming, and regenerating skeletal muscles of rat. Am. J. Physiol. Cell Physiol. 279: C639–C647. PMID:10942714.

Tokarska-Schlattner, M., Epand, R.F., Meiler, F., Zandomeneghi, G., Neumann, D., Widmer, H.R., et al. 2012. Phosphocreatine interacts with phospholipids, affects membrane properties and exerts membrane-protective effects. PLoS One, 7(8): e43178. doi:10.1371/journal.pone.0043178. PMID: 22912820.

Wallimann, T., Wyss, M., Brdiczka, D., Nicolay, K., and Eppenberger, H.M. 1992. Intracellular compartmentation, structure and function of creatine kinase isozymes in tissues with high and fluctuating energy demands: the 'phosphocreatine circuit' for cellular energy homeostasis. Biochem. J. 281: 21–40. PMID:1731757.

Wallimann, T., Tokarska-Schlattner, M., and Schlattner, U. 2011. The creatine kinase system and pleiotropic effects of creatine. Amino Acids, 40(5): 1271–1296. doi:10.1007/s00726-011-0877-3. PMID:21448658.